Int. J. Heat Mass Transfer. Vol. 24, No. 11, pp. 1833–1846, 1981
Printed in Great Britain

0017-9310/81/111833-14 $02.00/0

EFFECT OF REYNOLDS NUMBER ON A SLIGHTLY HEATED TURBULENT BOUNDARY LAYER

C. S. SUBRAMANIAN and R. A. ANTONIA
Department of Mechanical Engineering, University of Newcastle, N.S.W., 2308, Australia

(*Received* 16 *March* 1981 *and in revised form* 22 *May* 1981)

Abstract—Measurements in a slightly heated turbulent boundary layer, with essentially identical origins for momentum and thermal fields, indicate that the constants in the velocity and temperature logarithmic regions do not vary with Reynolds number. The extent of these regions, as a proportion of the boundary layer thickness, is approximately constant, independent of the momentum thickness Reynolds number R_m when $R_m \gtrsim 3100$. The deviation from the temperature logarithmic law in the outer layer is reasonably well described by expressions analogous to those which describe the velocity "wake". The maximum value of this deviation increases with R_m over the range 990–4750 but is approx. constant for $R_m > 4750$, and equal to about half the maximum velocity deviation. Distributions of r.m.s. velocity and temperature scale moderately well with wall variables in the inner part of the sublayer at all R_m. Scaling on outer flow variables is only approximately achieved when $R_m \gtrsim 3100$. The only noticeable effect of R_m on the turbulent Prandtl number and turbulence structure parameters is observed at the smallest Reynolds numbers investigated.

NOMENCLATURE

C, C_θ, empirical constants, equations (1), (2);
c_f, skin friction coefficient, $\tau_w/(\frac{1}{2}\rho U_1^2)$;
c_p, specific heat at constant pressure;
e, fluctuating voltage;
f, f_θ, functions defined by equation (13);
H, shape parameter $= \delta_1/\delta_2$;
h, h_θ, functions defined by equation (12);
k, thermal conductivity;
l, l_T, extents of velocity and temperature log-laws;
Pr, molecular Prandtl number, ν/γ;
Pr_t, turbulent Prandtl number $= [-\overline{uv}/(\partial U/\partial y)]/[-\overline{v\theta}/(\partial T/\partial y)]$;
Q_w, thermometric wall heat flux $= -\gamma(\partial T/\partial y)_{y=0}$;
R_m, momentum thickness Reynolds number $= U_1\delta_2/\nu$;
St, Stanton number, $Q_w/U_1(T_w - T_1) = U_\tau T_\tau/U_1(T_w - T_1)$;
T, mean temperature;
T_τ, friction temperature, Q_w/U_τ;
T^*, $= (T_w - T)/(T_w - T_1)$;
U, V, mean velocity components in x, y directions;
U_τ, friction velocity, $(\tau_w/\rho)^{1/2}$;
U^*, $= U/U_1$;
u, v, fluctuating velocities in x, y directions;
$-\overline{uv}$, kinematic Reynolds shear stress;
$\overline{u\theta}$, $\overline{v\theta}$, thermometric longitudinal and normal heat fluxes respectively;
w, w_θ, velocity and thermal "wake" functions, equations (7), (8);
x, y, co-ordinates: x, streamwise; y, normal to wall;
y^+, $= yU_\tau/\nu$;
α, β, velocity and temperature sensitivities of single hot wire, equation (3);
α_1, α_2, β_1, β_2, velocity and temperature sensitivities of X-wire, equation (4);
γ, thermal diffusivity $= k/\rho c_p$;
Δ, $\int_0^\gamma (U_1 - U)/(U_\tau)\,dy$;
Δ_T, $\int_0^\gamma (T - T_1)/(T_\tau)\,dy$;
δ, momentum layer thickness (distance from wall at which $U = 0.99\,U_1$);
δ_T, thermal layer thickness [distance from wall at which $T - T_1 = 0.01\,(T_w - T_1)$];
δ_1, displacement thickness $\int_0^\infty (1 - \rho U/\rho_1 U_1)\,dy$;
δ_2, momentum thickness $= \int_0^\infty (\rho U/\rho_1 U_1)(1 - U/U_1)\,dy$;
δ_h, enthalpy thickness $= \int_0^\infty (\rho U/\rho_1 U_1)(T - T_1)/(T_w - T_1)\,dy$;
θ, temperature fluctuation;
ν, kinematic viscosity;
ρ, density;
κ, von Kármán constant $= 0.41$, equation (1);
κ_θ, empirical constant analogous to κ, equation (2);
Π, Π_θ, wake parameters, equations (7), (8).

Subscripts

1, free stream value;
w, wall value;

θ, T, refer to quantities associated with the thermal field.

Superscripts

$'$, r.m.s. value;

$^+$, denotes normalization by wall variables.

$\bar{}$, denotes conventional time average.

1. INTRODUCTION

COLES [1] found that the velocity defect law in the outer part of a boundary layer in zero pressure gradient is independent of R_m ($= U_1\delta_2/\nu$, where U_1 is the free stream velocity, ν is the kinematic viscosity of the fluid and δ_2 is the momentum thickness) when R_m is greater than about 5000 but is a fairly strong function of R_m when $R_m < 5000$. Coles' analysis assumed the validity of the logarithmic velocity profile

$$\frac{U}{U_\tau} = \frac{1}{\kappa}\ln y^+ + C, \tag{1}$$

with $\kappa = 0.41$ and $C = 5.0$. Simpson [2] claimed that there is in fact no dependence of velocity on R_m, once allowance is made in (1) for the variation of κ with R_m. This claim was refuted by Huffman and Bradshaw [3] on the basis of their analysis of existing data on low Reynolds number flows. These authors suggested that the R_m dependence of the velocity defect may be attributed to the presence of the viscous superlayer, identified by Corrsin and Kistler [4], at the turbulent/irrotational interface since velocity defect profiles in fully developed pipe flow, where no such interface occurs, are Reynolds number independent. Bradshaw [5] argued that at the lower values of R_m, the thickness of the viscous superlayer is comparable to that of the viscous sublayer but, because the interface is highly contorted (smoke-flow visualization reveals increasing contortions as R_m decreases), the volume of the superlayer per unit plan area may be one order of magnitude larger than the actual thickness measured normal to the interface. Mean flow measurements by Murlis *et al.* [6] (see also Murlis [7]), Purtell *et al.* [8] and Purtell [9] have confirmed, for a turbulent boundary layer with zero pressure gradient, the validity of (1) with $\kappa = 0.41$ and $C = 5.0$–5.2. The dearth of turbulence measurements in low Reynolds number boundary layer with zero pressure gradient, the validity of (1) with $\kappa = 0.41$ and $C = 5.0$–5.2. The dearth range $700 < R_m < 5000$. These measurements included distributions of r.m.s. u and v intensities, the Reynolds shear stress and budgets of turbulent energy. Both conventional and conditional measurements were made. Purtell *et al*'s [8] investigation was aimed at extending the data base at low Reynolds numbers with emphasis on mean velocity and distributions of $\overline{u^2}$.

There are few measurements of the r.m.s. θ intensity and of longitudinal and normal heat fluxes in a thermal boundary layer where the origins of momentum and heat are nearly coincident. The present investigation provides mean and fluctuating velocity and temperature measurements in such a boundary layer over the range $990 < R_m < 7100$. The validity of the temperature logarithmic law

$$\frac{T_w - T}{T_\tau} = \frac{1}{\kappa_\theta}\ln y^+ + C_\theta \tag{2}$$

is investigated in Section 3 for this range of R_m. The Reynolds number dependence of the mean temperature defect law in the outer layer is also examined in Section 3. The applicability of the scaling, based on either inner or outer layer variables, of r.m.s. values of u and θ is discussed. Distributions of the turbulent Prandtl number, derived from measurements of U, T, $\overline{uv}$ and $\overline{v\theta}$, and of a few turbulence structure parameters, which describe dimensionless properties of the turbulence, are presented in Section 4.

2. EXPERIMENTAL ARRANGEMENT AND CONDITIONS

The experimental work has been carried out in the 0.38 × 0.25 m working section of an open return circuit blower wind tunnel. The centrifugal blower, driven by an 8.4 kW Siemens motor, supplies air to the working section via two 2-dim. diffusers, a settling chamber and a series of screens. A detailed description of the equipment and experimental arrangement may be found in Subramanian [10]. The maximum speed in the working section is about 20 ms^{-1}. The roof of the working section is adjusted to provide approximately a constant pressure (within $\pm 2\%$) for the present range of U_1. The first 3 m of the working section floor consist of 20 identical heated Inconel strips (0.46 mm × 0.15 m × 0.38 m) supported by five Sindanyo (hard asbestos boards) base plates. The strips are insulated from each other and connected in series to provide a uniform wall heat flux distribution. A.C. heating is used with a transformer operated at 60 V, and between 45 and 90 amps. The last 1.83 m of the test section floor are unheated and consist of epoxy coated Sindanyo board. The heated section is fitted with Copper Constantan thermocouples, located at several streamwise and spanwise stations. The thermocouple cold junctions are kept approximately at the free stream temperature (typically 22 ± 1°C) over the duration of the experimental runs. The thermocouple e.m.f. was measured with a Cambridge potentiometer. The plate was continuously heated from the beginning of the working section to about 14°C above ambient at 2.2 m from the trip. A 3 mm dia. wire was placed on the heated wall, 40 mm from the entrance of the test section, to trip the boundary layer. The location of the trip was determined by a trial and error method in which the momentum thickness δ_2 and enthalpy thickness δ_h were compared at different distances from the trip and for different free stream speeds. The magnitudes of δ_2 and δ_h were approximately (within

$\pm 1.5\%$) equal at all values of R_m. For the finally chosen location of the trip, the origins of the aerodynamic and thermal layers coincided to within ± 25 mm.

All velocity measurements were made with a single hot wire (Pt-10% Rh, 5 μm dia., 1 mm length), operated by a DISA 55M10 constant temperature anemometer at a resistance ratio of 1.8. Temperature measurements were made with a 0.8 mm long, 0.63 μm dia. Pt-10% Rh cold wire (temperature coefficient, obtained by measurement, was $1.5 \times 10^{-3}\,^{\circ}\mathrm{C}^{-1}$) operated by a constant current anemometer. For a current value of 50 μA, and the present experimental conditions, the velocity sensitivity of the cold wire was negligibly small (typically $0.006^{\circ}\mathrm{C/ms}^{-1}$). No compensation was made for the thermal inertia of the cold wire. The response of the wire to the crossing of the turbulent/irrotational interface in the outer part of the boundary layer was observed on a storage oscilloscope. Adjustment of the setting of a compensator (designed to give a frequency response that is flat up to 20 kHz) did not improve the response of the wire as the decrease, at the upstream interface, of the temperature to its background value was generally sharp at all speeds examined. (The use of a 1 μm cold wire by Antonia *et al.* [11] did require the use of the compensator). After suitable conditioning, a signal proportional to the instantaneous temperature was recorded on a 4-channel Hewlett-Packard (3960A) analogue FM tape recorder at a speed of 0.38 ms^{-1}. Analogue records were typically of about 150 s duration.

The quantities, $\overline{uv}$, $\overline{u\theta}$, $\overline{v\theta}$ were obtained with an X-wire/cold wire arrangement, with the cold wire located 1.23 mm upstream of the geometrical centre of the X-array and in a direction perpendicular to the plane of the X-array. The X-wire/cold wire arrangement was initially calibrated for velocity and temperature in the heated core of a plane jet. The X-probe (the hot wire resistances were matched to within 1%) was operated by two DISA 55M10 anemometers and DISA 55M25 linearisers. The contamination of the velocity signal by temperature was removed using a technique identical to that described by Champagne [12].

The instantaneous linearised voltage of a single hot wire is a function of the instantaneous velocity and temperature respectively. The fluctuating voltage e can be written (the maximum value of u'/U in the present experiments is about 0.2) as

$$e = \alpha u + \beta\theta \tag{3}$$

where $\alpha = \partial E/\partial U$ and $\beta = \partial E/\partial T$. By analogy, the X-wire voltages may be written

$$\begin{aligned} e_1 &= \alpha_1(u + v\cot\psi_1) + \beta_1\theta \\ e_2 &= \alpha_2(u - v\cot\psi_2) + \beta_2\theta. \end{aligned} \tag{4}$$

The constants α_1, α_2, ψ_1 and ψ_2 (effective inclinations of the hot wires to the free stream direction) are found by calibrating the hot wires in the isothermal stream for different speeds, and different yaw angles, while β_1 and β_2 are found by varying the temperature of the jet for a given speed and with zero yaw. In the present case, $\alpha_1 = \alpha_2$ and $\beta_1 = \beta_2$. The digital time series corresponding to the fluctuating temperature sensor voltage was shifted in time to correct for the longitudinal separation between the X-wire and the cold wire. Signals from the temperature arrangement were recorded on an 8-channel FM tape recorder (HP3968A) at a speed of 0.38 ms^{-1} and subsequently digitised at frequencies in the range 2–20 kHz, the lower and upper bounds of this range corresponding to the lowest and highest values of U_1 respectively, after appropriate reduction in the playback speed of the tape. Signals proportional to u and v were obtained from the X-wire/cold wire voltages using analogue computer elements. Digital records were stored on magnetic tapes and discs before processing on a DEC PDP 11/34 computer.

The growths of thermal and momentum layers were found to be identical to within $\pm 3\%$ and proportional to $x^{0.79}$ (x is the distance from the trip) at U_1 of 4.1 and 14.7 ms^{-1}. Most of the measurements were made at 2.24 m from the trip for values of U_1 of 2.1, 4.1, 8.4, 12.6, 16.7 and 18.8 ms^{-1}. A set of measurements was made at a constant U_1 (14.7 ms^{-1}) but at different x (0.54, 1.01, 1.91, 2.24 and 2.83 m). The skin friction coefficient c_f was determined from a Preston tube (two diameters 0.6 and 1.22 mm, were used). The wall heat flux Q_w, was estimated from the slope of the temperature profile in the linear sublayer. This profile was found to be linear up to $y^+ \simeq 10$. The Wollaston wire was bent, before etching, into a U-shape to enable measurements of temperature in this region. The wall heat flux was determined with reasonable accuracy ($\pm 5\%$), even at large values of R_m when the viscous sublayer is relatively thin. At $x = 2.24$ m, measured values of Q_w and c_f in the z direction were constant to within $\pm 2\%$ over a distance $z/\delta \simeq \pm 1.6$. A summary of experimental conditions at $x = 2.24$ m is given in Table 1.

3. MEAN VELOCITY AND TEMPERATURE RESULTS AND DISCUSSION

Mean velocity profiles measured with the hot wire are plotted in semi-logarithmic form in Fig. 1. Profiles obtained with the pitot tube were in reasonable agreement with those obtained with the hot wire. At all R_m, the profiles are in agreement of (1) with $\kappa \simeq 0.41 \pm 0.01$ and $C = 5.2 \pm 0.2$. It should be noted that the values of U_τ used in Fig. 1 were obtained with Preston tubes using the calibration of Patel [13] (and the simplified expressions given by Head and Ram [14]). As the validity of the preston tube calibration at low R_m has not been directly established in the present experiment, the constancy of κ and C with R_m should receive some qualification. Murlis *et al.* [6] have reported good agreement between the Preston tube (with Patel's calibration) and the Stanton tube for values of R_m extending down to 700. Since the Stanton

Table 1. Summary of mean flow data at $x = 2.24$ m

U_1 (ms^{-1})	R_m	δ (cm)	δ_T (cm)	δ_1 (cm)	δ_2 (cm)	H $(=\delta_1/\delta_2)$	$2St/c_f$	Δ (cm)	Δ_T (cm)	T_t (°C)	U_τ (ms^{-1})	$T_w - T_1$ (°C)
2.12	990	5.4	5.4	1.02	0.68	1.50	1.51	19.7	14.6	0.83	0.10	12.2
4.1	1500	4.5	4.6	0.78	0.53	1.47	1.50	18.2	12.4	0.90	0.18	13.9
8.44	3100	4.7	4.4	0.82	0.54	1.52	1.53	20.7	11.6	0.85	0.33	14.0
12.64	4750	4.5	4.7	0.78	0.54	1.42	1.53	21.1	12.3	0.73	0.46	13.0
16.73	6500	4.7	4.8	0.80	0.57	1.41	1.40	21.5	13.0	0.66	0.62	12.7
18.81	7100	4.8	4.8	0.73	0.55	1.35	1.40	20.0	13.7	0.65	0.69	12.7

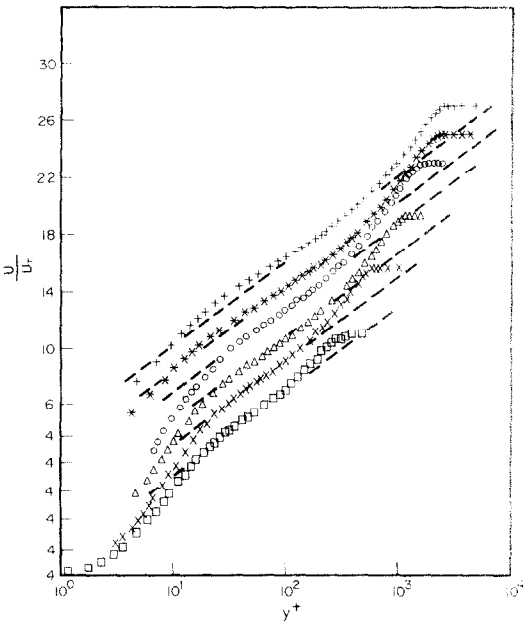

FIG. 1. Mean velocity profiles in semi-logarithmic coordinates. Ordinate scale refers to highest curve; other curves successively displaced downwards by 2 units. □, $R_m = 990$; ×, 1500; △, 3100; ○, 4750; *, 6500; +, 7100.

tube is submerged within the linear sublayer, its reading is not expected to reflect the influence, if it indeed exists, of Reynolds number for small values of R_m. It seems therefore reasonable to interpret Fig. 1 as providing further support for Murlis *et al.*'s [6] and Purtell *et al.*'s [8] finding that κ and C are not affected by Reynolds number or equivalently, that reliable use can be made of the Clauser chart technique, with $\kappa = 0.41$ and $C = 5.0$–5.4, at all values of R_m^*. The present Preston tube values of c_f are in good agreement (Fig. 2) with those obtained by Murlis *et al.* and Purtell *et al.*

Mean velocity profiles obtained for $U_1 = 14.7$ ms^{-1}, but for different values of x, also show agreement with (1) in the inner layer but exhibit, at relatively small values of $x (x \leq 1$ m), a wake region which is significantly smaller than that in Fig. 1 for corresponding values of R_m. This difference reflects the influence of the trip rod. Klebanoff and Diehl [15] found that, close to the trip, the velocity profile is considerably influenced by the trip and a minimum distance of 450 times the size of the trip was necessary before this influence disappeared. While Graham [16] suggested that a distance of 100 trip heights is required before a normal "wake" is established, the present investigation indicates that a distance of approx. 300 trip diameters is needed to establish a normal "wake". The settling distance is expected to depend on the location of the trip (more accurately on the ratio of the trip size to boundary layer thickness) and on the free

* R_m must of course be sufficiently high for the flow to be fully turbulent.

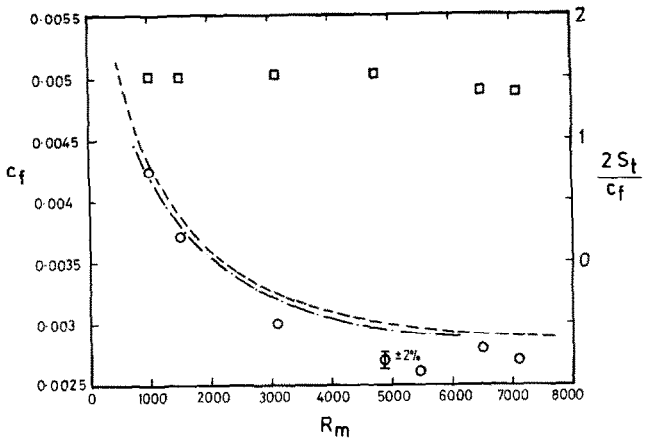

FIG. 2. Variation of skin friction coefficient and Reynolds analogy factor with Reynolds number. c_f: ○, present; – · –, best to fit to data of Murlis *et al.*; – – –, Coles' distribution. $2St/c_f$, □.

stream turbulence level. A decrease in the "wake" strength occurs when the free stream turbulence intensity is greater than 0.2% (e.g. Ahmad *et al.* [17]; Simonich and Bradshaw [18]). For the present investigation the measured free stream turbulence level decreased from about 0.2% at $R_m \simeq 990$ to about 0.1% at $R_m \simeq 7100$.

Semi-logarithmic plots of mean temperature profiles in Fig. 3 indicate that κ_θ and C_θ in relation (2) are, on average, constant and equal to 0.48 ± 0.02 and 2.0 ± 0.2 respectively. Since the values of T_τ used in Fig. 3 depend on U_τ, the independence of κ_θ and C_θ with Reynolds number must be qualified in the same manner as the independence of κ and C. The constant κ_θ is often (e.g. Kader and Yaglom [19]) assumed to be given by

$$\kappa_\theta = \frac{\kappa}{Pr_t}. \tag{5}$$

Since the turbulent Prandtl number is defined as

$$Pr_t = \frac{\overline{uv}/(\partial U/\partial y)}{\overline{v\theta}/(\partial T/\partial y)}, \tag{6}$$

the use of (1) and (2) in (6) leads to (5) only if either $-\overline{uv}$ and $\overline{v\theta}$ are constant (equal to U_τ^2 and $U_\tau T_\tau$, respectively) over the logarithmic region or the ratios $-\overline{uv}/U_\tau^2$ and $\overline{v\theta}/U_\tau T_\tau$ have identical values at the same value of y^+. Present measurements, presented in Section 4, and those of Fulachier [20] (obtained with a small unheated starting length) indicate that, in the inner layer, $\overline{v\theta}/U_\tau T_\tau$ decreases more rapidly than $-\overline{uv}/U_\tau^2$ with increasing y. The present value of 0.85 for the ratio κ/κ_θ is only slightly smaller than the value

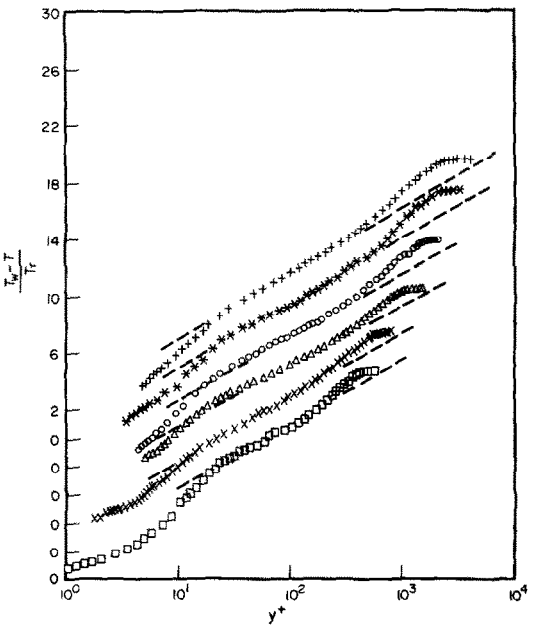

FIG. 3. Mean temperature profiles in semi-logarithmic coordinates. Ordinate scale refers to highest curve; other curves successively displaced downwards by 2 units. Symbols are as in Fig. 1.

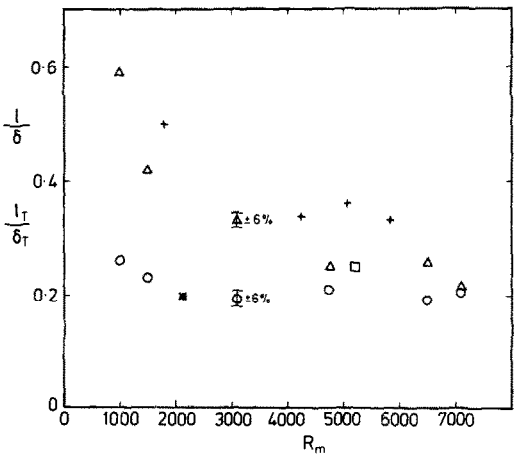

FIG. 4. Extent of velocity and thermal logarithmic regions as a fraction of the boundary layer thickness. ○, velocity; △, temperature; +, Perry and Hoffmann; *, Orlando *et al.*; □, Fulachier.

of 0.87 suggested by Yaglom [21]. Fulachier [20] obtained values for κ_θ and C_θ of 0.45 and 3.1 respectively at $R_m \simeq 5000$, whereas Perry and Hoffmann [22] (identical origins for momentum and thermal layers) assumed the values suggested by Kader and Yaglom [19] ($\kappa_\theta = 0.45$; $C_\theta = 3.3$) for a "thermal" Clauser chart determination of Q_w. To within the experimental uncertainty, the present value of C_θ is in good agreement with that obtained by Antonia *et al.* [23] well downstream of a sudden increase in surface heat flux but is smaller than previous estimates of C_θ. Yaglom [21] mentions that C_θ, which depends on Pr, is rather difficult to determine but the scatter in C_θ is no larger than the scatter in C.

The extents l and l_T of the velocity and temperature logarithmic regions were inferred from the straight line portions of Figs. 1 and 3 and are plotted in Fig. 4 as a function of Reynolds number. Expressed as a function of δ, l decreases slowly as R_m increases up to about 3100. The ratio l/δ remains approx. constant for $R_m >$ 3100 and its magnitude is only slightly larger than the values of Purtell *et al.* [8] which are in the range 0.15–0.2. These authors indicated that for smaller R_m, l/δ may increase slightly but no definite conclusion was drawn because of the scatter in the data. For $R_m <$ 4750, the increase of l_T/δ_T with decreasing R_m is more pronounced than the increase of l/δ. The present trend for l_T/δ_T is in good agreement with that deduced from the data of Perry and Hoffman [22]. However, l^+ ($\equiv lU_\tau/\nu$) and l_T^+ show a linear increase with R_m and the extent of l_T^+ is, on average, about 70% greater than l^+.

Similarity on outer layer variables of the mean velocity and temperature profiles is tested in Figs. 5 and 6, when the thickness Δ, introduced by Rotta [24], and its thermal analogue Δ_T are used as the normalizing length scales. It follows from the definition of Δ and Δ_T that the areas under the curves in Figs. 5 and 6 are equal to unity. The ratio of Δ/Δ_T, which may be inferred from Table 1, ranges from 1.35 to 1.78. The deviation from unity of this ratio was attributed by Perry and Hoffmann [22] to a breakdown of the Reynolds analogy. The outer layer scaling of the profiles seems adequate, at all Reynolds numbers,

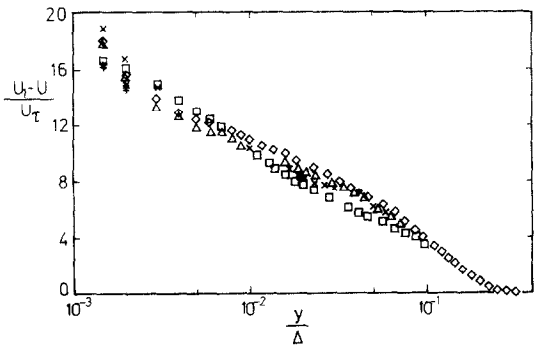

FIG. 5. Mean velocity defect. □, R_m = 990; ×, 1500; △, 3100; ◇, 4750; *, 6500; +, 7100. Where symbols overlap only one symbol is shown.

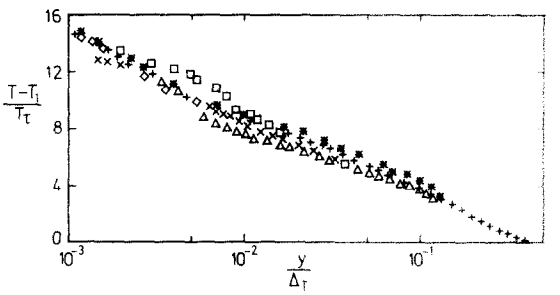

FIG. 6. Mean temperature defect. Symbols are as in Fig. 5.

when y/Δ (or y/Δ_T) is greater than 0.1. At $R_m = 990$ and 1500 and when $y/\Delta < 0.1$, the departure of the velocity defect in Fig. 5 from the trend followed by all the data for $R_m \geq 3100$ is fairly evident. Any deviation of the temperature defect at $R_m = 990$ and 1500 in Fig. 6 is not easy to distinguish, suggesting that outer layer scaling seems to be valid for the mean temperature field at all values of R_m (within experimental scatter).

Mean velocity and temperature distributions in the outer layer may be written as

$$\frac{U}{U_\tau} = \frac{1}{\kappa}\ln y^+ + C + \frac{\Pi}{\kappa} w(y/\delta), \tag{7}$$

$$\frac{T_w - T}{T_\tau} = \frac{1}{\kappa_\theta}\ln y^+ + C_\theta + \frac{\Pi_\theta}{\kappa_\theta} w_\theta(y/\delta_T), \tag{8}$$

where w and w_θ are velocity and thermal "wake" functions respectively and Π and Π_θ are "wake" parameters which reflect the strengths of these "wakes". The third term on the right sides of (7) and (8) represent deviations from the logarithmic laws (1) and (2) and are shown plotted in Figs. 7 and 8 as functions of y/δ and y/δ_T^+. Also shown in Fig. 7 are the deviations corresponding to Coles' [1] tabulation of the wake function $w(y/\delta)$ and Dean's [25] semi-empirical formula

$$\frac{\Pi}{\kappa} w(y/\delta) = \frac{1}{\kappa}(1 + 6\Pi)(y/\delta)^2 - \frac{1}{\kappa}(1 + 4\Pi)(y/\delta)^3. \tag{9}$$

Both (9) and Coles' wake function satisfy the conditions $w(1) = 2$ and $w(0) = 0$. In addition, (9) satisfies the conditions that at $y = 0$ and $y = \delta$ the derivatives of w with respect to y/δ are equal to zero and $-1/\kappa$ respectively. Coles' tabulation represents the data more satisfactorily than (9), except perhaps at $R_m =$

† Note that the use of δ or δ_T, which are readily available in the literature, cannot be regarded as equivalent to using Δ or Δ_T since the proportionality between δ and Δ or between δ_T and Δ_T depends on R_m.

‡ The present range of R_m did not extend to sufficiently large enough values to substantiate Mabey's [26] finding that the wake component reaches a maximum about $R_m = 6000$ before decreasing slowly. Mabey found that the maximum was significantly higher at supersonic than at subsonic speeds. Mabey's results that the wake component is zero at $R_m \simeq 600$ differs from Coles' tabulation for $2\Pi/\kappa$ which indicates the disappearance of the wake at $R_m \simeq 460$ and Purtell *et al.*'s [8] finding that a substantial deviation still exists at $R_m \simeq 460$.

990. In analogy to (9), the thermal wake function can be written as

$$\frac{\Pi_\theta}{\kappa_\theta} w_\theta(y/\delta_T) = \frac{1}{\kappa_\theta}(1+6\Pi_\theta)(y/\delta_T)^2 - \frac{1}{\kappa_\theta}(1+4\Pi_\theta)(y/\delta_T)^3 \quad (10)$$

with boundary conditions analogous to those for the velocity wake function. Expression (10) yields a satisfactory representation of the data (Fig. 8) at least for the three higher Reynolds numbers considered here and for values of y/δ extending up to about 1. At $R_m =$ 3100 and 1500, an expression similar to Coles' wake function is in slightly better agreement with the data than (10). The extent of the thermal wake at $R_m = 990$ is too small to allow meaningful comparison with (10) or Coles' wake function.

Maximum deviations of mean velocity and mean temperature in the outer layer from the logarithmic distributions are given by $2\Pi/\kappa$ and $2\Pi_\theta/\kappa_\theta$ respectively. These deviations characterise the strengths of the "wakes" and are shown plotted in Fig. 9 as a function of R_m. The present values of $2\Pi/\kappa$ are in reasonable agreement with Coles' [1] proposed asymptotic function (shown in Fig. 9) and the more recent results of Murlis *et al.* [6] and Purtell *et al.* [8]. The present distribution of $2\Pi_\theta/\kappa_\theta$ exhibits the same qualitative behaviour‡ as $2\Pi/\kappa$, increasing in magnitude with increasing R_m and reaching an approximately constant value for $R_m \gtrsim 5000$ of about 1.4, approx. half the value of $2\Pi/\kappa$ over this Reynolds number range. This maximum value for $2\Pi_\theta/\kappa_\theta$ is in good agreement with the values inferred from the data of Perry and Hoffmann [22] and Perry *et al.* [27]. It is a little smaller than the value of about 1.9 obtained by

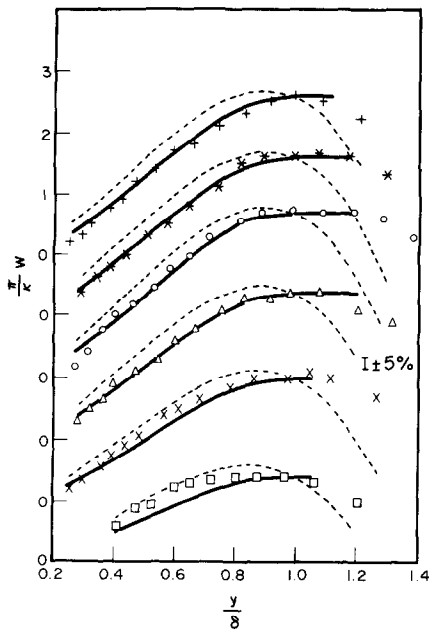

FIG. 7. Velocity "wake" distribution. Symbols are as in Fig. 1. – – –, equation (9); ——, Coles.

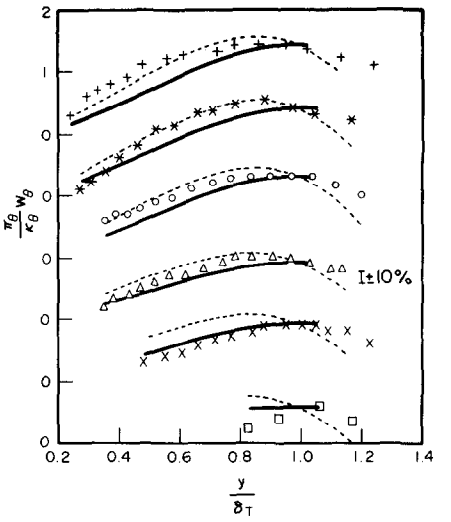

FIG. 8. Thermal "wake" distribution. Symbols are as in Fig. 1. – – –, equation (10); ——, Coles.

Simonich and Bradshaw [18] at $R_m \simeq 6000$. Zukauskas and Slanciauskas' recommendation (reported by Yaglom [21]) of 1.5 for $2\Pi_\theta/\kappa_\theta$ is in good agreement with the present value.

For $R_m < 3100$, the present values of $2\Pi_\theta/\kappa_\theta$ decrease more slowly than the values inferred from Perry and Hoffmann's data or Orlando *et al*'s [28] data. The relatively rapid decrease ($R_m < 3100$) of Perry and Hoffmann's Π_θ values may be partly attributed to the presence of a slight favourable pressure gradient. It should also be noted that, as in Murlis *et al.*'s [8] study, the R_m variation in Perry and Hoffmann's experiment was achieved by varying x. Perry and Hoffmann's mean temperature profile at $R_m = 1790$ indicates a negative value of Π_θ.

The present distributions of $2\Pi/\kappa$ and $2\Pi_\theta/\kappa_\theta$ at low values of R_m do not preclude the possibility that both velocity and thermal wakes may disappear at approximately the same Reynolds number. The decreasing magnitude of the difference $(\Pi_\theta - \Pi)$ when R_m is less than 3100 may have a direct effect on the Stanton number St and on the Reynolds analogy factor $2St/c_f$. An expression for $2St/c_f$ can be easily obtained from

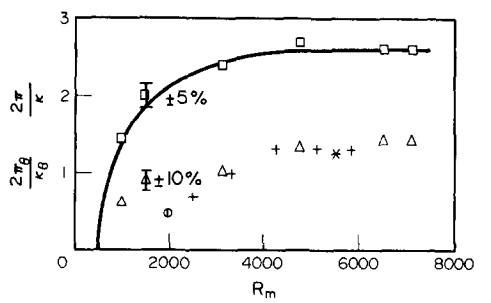

FIG. 9. Variation of velocity and thermal wake strengths with Reynolds numbers. $2\Pi/\kappa$: □, present data with $C = 5.2$; ——, Coles' best fit to the data. $2\Pi_\theta/\kappa_\theta$: △, present data with $C_\theta = 2.0$; ○, Orlando *et al.*; *, Perry *et al.*; +, Perry and Hoffmann.

(7) and (8). Evaluation of (7) and (8) at $y = \delta (U = U_1;$ $T = T_1)$ and elimination of $\delta U_e/\nu$ from these equations yields (e.g. Simonich and Bradshaw [18])

$$\frac{2St}{c_f} = \frac{\kappa_\theta/\kappa}{1 + I\sqrt{(c_f/2)}} \tag{11}$$

where

$$I \equiv \frac{C_\theta \kappa_\theta - C\kappa + 2(\Pi_\theta - \Pi)}{\kappa}.$$

The present trend for the difference $(\Pi_\theta - \Pi)$ could suggest that the increase in $\sqrt{(c_f)}$ for $R_m < 1500$ is not accompanied by a proportional increase in the ratio $2St/c_f$. The increase in c_f in the denominator of (11) is, to some extent, offset by a decrease in $I(<0$, since $C\kappa > C_\theta \kappa_\theta$ and $\Pi_\theta < \Pi)$. For the present values of the constants C, C_θ, κ, κ_θ and of the parameters Π_θ, Π, the ratio $2St/c_f$ decreases only slightly from about 1.41 at $R_m \simeq 990$ to 1.36 at $R_m \simeq 7100$. Experimental values of $2St/c_f$, shown in Table 1, vary between 1.54 and 1.4. Although the effect of free stream turbulence level on the boundary layer is outside the scope of the present investigation, mention should be made of Simonich and Bradshaw' s finding of the dissimilar variations of Π and Π_θ with increasing turbulence level u'/U_1. As this level is increased from 0.3 to 4.7%, $2\Pi/\kappa$ decreases monotonically from 2.6 to zero but $2\Pi_\theta/\kappa_\theta$, following an initial decrease, remains constant when u'/U_1 exceeds 0.025.

The plot of T^* $(\equiv T_w - T/T_w - T_1)$ vs. U^* $(\equiv U/U_1)$ in Fig. 10 shows that, at all values of R_m, the data follow the straight line $T^* = U^*$ for values of U^* or T^* greater than about 0.5. Pimenta *et al.* [29] presented plots of T^* vs. U^* for boundary layers over rough walls with and without blowing. They also compared these plots with a profile obtained by Blackwell *et al.* [30] over a smooth wall. The smooth wall profile appears to follow the distribution $T^* = U^*$ across the whole layer. Although the rough wall profiles also exhibit a linear distribution over most of the layer, its slope is equal to 0.85 (these authors suggested that a temperature jump condition exists at the wall). Orlando *et al.* [28] attributed the divergence between rough and smooth wall results in the region near the wall to the dominance of molecular transport close to the smooth wall surface. The equality $T^* = U^*$ follows from the mean momentum and enthalpy equations for a zero pressure gradient boundary layer only when certain specific conditions are satisfied. In particular, the origins for the momentum and thermal layers should coincide and both molecular and turbulent Prandtl numbers should equal unity. The validity of the eddy viscosity and eddy diffusivity concepts is implicit in the last requirement. Orlando *et al.* [28] noted that, for their rough surfaces, the momentum and thermal layers could not be forced to have the same virtual origin. The present experiment meets the requirement of a common virtual origin. The difference between boundary conditions for heat and momentum transfer can be attributed to

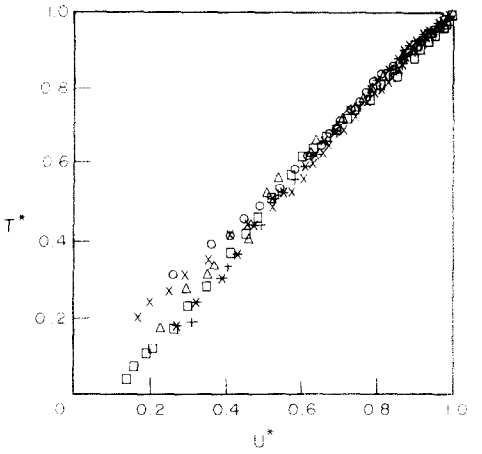

FIG. 10. Mean temperature versus mean velocity. Symbols are as in Fig. 1.

the influence of Pr on heat conduction at the boundary and is probably responsible for the deviation of the data in Fig. 10 from the relation $T^* = U^*$ in the region near the wall. In the remaining part of the layer, $Pr_t \simeq 1$ is at best a rough approximation and the molecular Prandtl number is not expected to play a significant role, at least at large values of R_m. It may be argued that, as R_m decreases, the increased importance of the superlayer could lead to an increased influence of the molecular Prandtl number in the outer layer. Such an influence is not evident in the results of Fig. 10.

4. VELOCITY AND TEMPERATURE FLUCTUATIONS

Similarity scaling for turbulent boundary layers suggests that, close to the wall, r.m.s. values of u and θ are given by

$$\frac{u'}{U_\tau} = h(y^+) \tag{12a}$$

and

$$\frac{\theta'}{T_\tau} = h_\theta(y^+) \tag{12b}$$

where h and h_θ are universal functions. In the outer

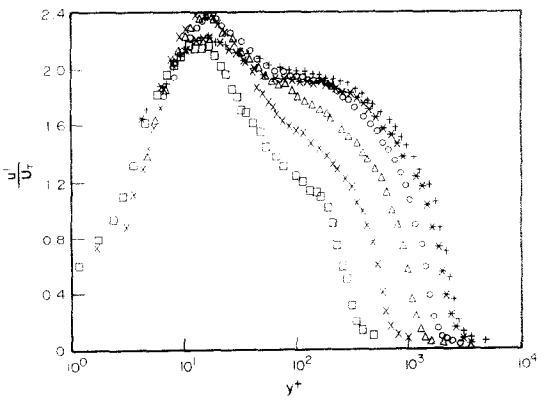

FIG. 11. Reynolds number variation of distribution of r.m.s. longitudinal velocity, with scaling on wall variables. Symbols are as in Fig. 1.

flow region, self-preservation suggests that

$$\frac{u'}{U_\tau} = f(y/\Delta) \tag{13a}$$

and

$$\frac{\theta'}{T_\tau} = f_\theta(y/\Delta_T). \tag{13b}$$

The present distributions of u' and θ' across the boundary layer are plotted in Figs. 11 and 12 using wall variables and in Figs. 13 and 14 using outer flow scaling. Figure 11 indicates reasonable similarity of u' up to about $y^+ \simeq 10$. Although the maximum value of u'/U_τ occurs at $y^+ \simeq 15$, the scatter in the maximum value of u'/U_τ is significant (2.1–2.4) and does not permit a definite conclusion with regard to the influence of R_m on distributions of u' over the logarithmic region. For $R_m = 990$, u' decreases fairly rapidly with y^+ after the maximum is reached while for $R_m \geq 4750$, u' decreases relatively slowly over a significant part of the logarithmic region. Similarity of θ' on wall variables appears to extend (Fig. 12) to larger values of y^+ than for u' but the maximum value of θ'/T_τ occurs at approximately the y^+ location at which u'/U_τ is maximum. The outer layer scaling in Fig. 13 indicates reasonable similarity for $R_m \geq 3100$ in the outer part of the layer. Temperature profiles in Fig. 14 also exhibit similarity at a large value of R_m, distributions at $R_m \leq 3100$ differing markedly from those for $R_m > 3100$. Using smooth walled pipe flow data, Perry and Abell [31] proposed a region of overlap between an inner scaling, as given by (12a), and outer scaling, (13a), which leads to a universal value of u'/U_τ in the wall region of the flow. Perry and Hoffmann [22] indicated that while similar arguments would, at first sight, indicate that u'/U_τ should be constant over the logarithmic region of a turbulent boundary layer, the energy-containing region of spectra in a turbulent boundary layer need not scale with U_τ and y alone (experimental evidence showing the influence of the inactive motion was given by Bradshaw [32]) suggesting more complicated scaling laws in boundary flow. The boundary layer distributions of u'/U_τ, obtained by Perry and Hoffmann, did not indicate a region where u'/U_τ is constant; however, these authors noted the presence of a knee in these distributions at a value of $u'/U_\tau \simeq 2.2$. Perry and Abell [33] indicated that such a simple scaling law is not valid and, from spectral considerations, proposed that broad-band turbulence intensity profiles should possess a logarithmic singularity. Further supporting evidence for this proposal has been given by Henbest *et al.* [34]. The distributions of Fig. 11 suggest that a knee occurs when u'/U_τ is in the range 1.9–2.0 but seem to indicate that $u'/U_\tau =$ constant may be a good approximation at large values of R_m.

Yaglom [21] extended the simple scaling law of Perry and Abell [31] to high order moments of velocity and scalar (temperature and concentration) fluctuations. In the latter case, he showed that the ratio $\overline{\theta^n}/T_\tau^n$ is expected to be constant over a region which corresponds approximately (at least when $Pr_t \simeq 1$) with that over which $\overline{u^n}/U_\tau^n$ is expected to be constant. Yaglom indicated that existing data on moments of θ are somewhat unreliable and suggested that the discrepancy between atmospheric and laboratory values of $\overline{\theta^2}/T_\tau^2$ may reflect the influence of Reynolds number. The present distributions of θ'/T_τ seem to suggest that a plateau region would be attained, if at all, at much higher values of R_m than for u'/U_τ. A knee at $\theta'/T_\tau \simeq 1.5$ is evident for the larger values of R_m (Fig. 12).

The normalized Reynolds shear stress $-\overline{uv}/U_\tau^2$ (Fig. 15) is approx. equal to unity in the logarithmic region $0.05 < y/\delta < 0.2$, and exhibits good similarity in the outer part of the layer over the complete Reynolds number range. The Reynolds shear stress data of Murlis [7] can be interpreted to be in agreement with the present distribution as no obvious dependence on R_m can be detected. The present values of $-\overline{uv}/U_\tau^2$ are in close agreement with those of Pimenta *et al.* [29] but are larger than those obtained by Klebanoff [35] for $R_m = 7800$. Reynolds shear stress measurements made with the wall unheated were in good agreement with

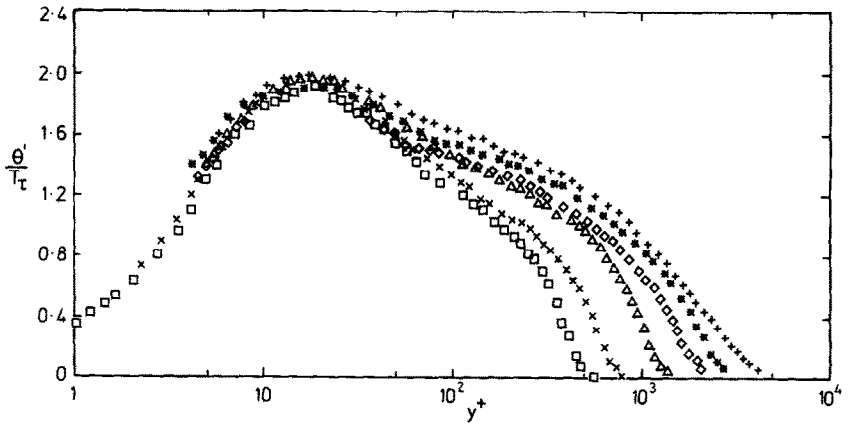

FIG. 12. Reynolds number variation of distributions of r.m.s. temperature, with scaling on wall variables. Symbols are as in Fig. 5.

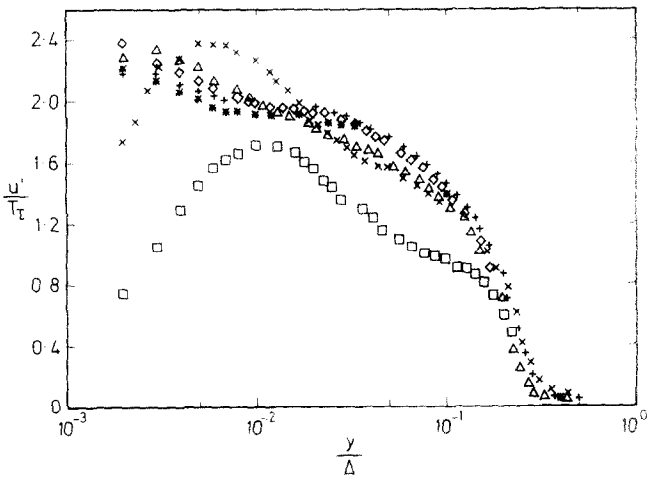

FIG. 13. Distributions of r.m.s. velocity, with scaling on outer flow variables. Symbols are as in Fig. 5.

those made with the heated wall providing good support for the suggestion made earlier that the temperature is a passive marker of the flow.

Like the $-\overline{uv}/U_\tau^2$ profiles, distributions of $\overline{v\theta}/U_\tau T_\tau$ (Fig. 16) exhibit good similarity over most of the layer for $R_m \geq 4750$. However, in contrast to the trend for $-\overline{uv}/U_\tau^2$, $\overline{v\theta}/U_\tau T_\tau$ is not constant in the log region, at least at the larger values of R_m, but shows a continuous decrease with increasing distance from the wall. For $R_m < 4750$, the magnitude of $\overline{v\theta}/U_\tau T_\tau$ shows a systematic decrease with decreasing R_m. Although different experimental runs confirmed the reproducibility of this trend, it seems difficult to reconcile the near wall magnitude of $\overline{v\theta}$ (Fig. 16) at the three smaller values of R_m with the expectation, based on a consideration of the mean enthalpy equation, that the gradient of the total heat flux $(\overline{v\theta} - \gamma\partial T/\partial y)$ should approach zero as y approaches zero. The molecular contribution to the total flux is negligible at $y/\delta = 0.1$ and cannot explain the departure of the lower R_m distributions of $\overline{v\theta}$ from those at higher R_m. Fulachier's measurements of $\overline{v\theta}$ at $R_m \simeq 5000$ are in reasonable agreement (Fig. 16) with the present distributions. Blom [36] presented measurements of $\overline{v\theta}$ at two values of U_1 corresponding to $R_m \simeq 1400$ and 2000. Although Blom's values (only those at $R_m \simeq 2000$ are shown in Fig. 16) are in closer agreement with Fulachier's values or the present measurements at the larger R_m, a correction factor was applied by Blom to $\overline{v\theta}$ (and also to $-\overline{uv}$). This correction was determined by matching the maximum measured value of $\overline{v\theta}$ with that calculated, using the mean enthalpy equation, from the measured mean velocity and mean temperature profiles. Corrected values (shown in Fig. 16) of $\overline{v\theta}$ were approx. 50% larger than the measured values. The need for such a correction was attributed to the non-uniform distribution of velocity and temperature fields along the length of the wires. For Blom's X-wire/cold wire geometry, the cold wire was perpendicular to the heated plate and parallel to the plane of the X-wire. Values of u' and θ' obtained from this geometry were 10–14% (apparently independent of y/δ) smaller than

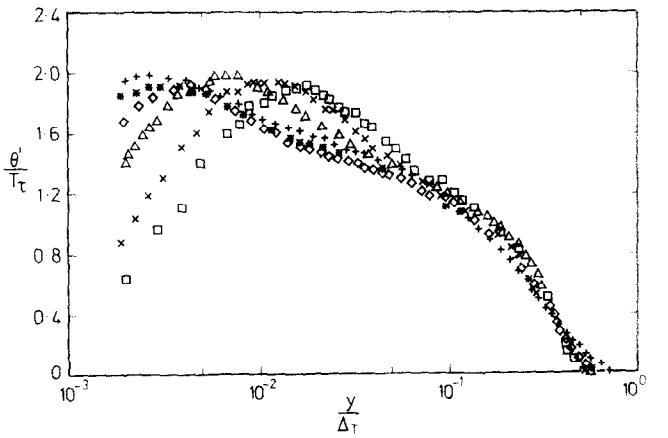

FIG. 14. Distributions of r.m.s. temperature, with scaling on outer flow variables. Symbols are as in Fig. 5.

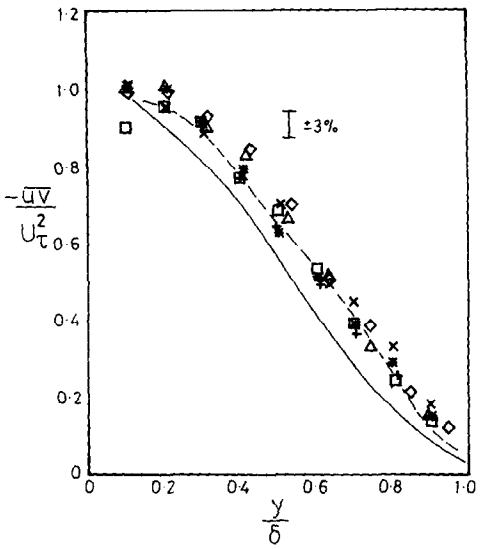

FIG. 15. Reynolds shear stress distributions. Symbols are as in Fig. 5. ——, Klebanoff; – – –, Pimenta *et al.*

those obtained with single wires oriented in the spanwire direction, parallel to the wall. While Blom argued that this discrepancy provided some justification for correcting $\overline{v\theta}$ and $\overline{uv}$, the present X-wire values of u' agreed (to better than 5%) with those from a single wire. Further, since the present distributions of $-\overline{uv}/U_\tau^2$ were found to be in close agreement with those calculated from the mean momentum equation, the application of a correction to $\overline{v\theta}$ of the kind used by Blom did not seem justifiable. A correction due to the physical separation between the cold wire and the centre of the X-wire was however, as noted earlier, applied to all present measurements of $\overline{v\theta}$ and $\overline{u\theta}$. This correction only amounted to about 2–3%.

Distributions of $\overline{u\theta}/U_\tau T_\tau$ (Fig. 17) are almost independent of R_m and although they are qualitatively similar to Fulachier's values, they are smaller than the

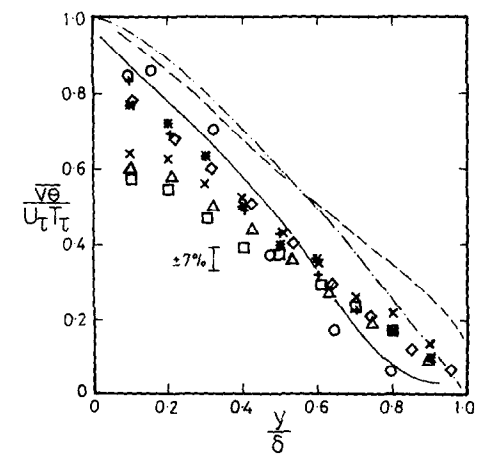

. 16. Normal heat flux distributions. Symbols are as in 5. ——, Fulachier; – – –, Orlando *et al.*; – · – · –, Calcu- 1 from mean enthalpy equation ($R_m = 4750$). ○, Blom ($R_m \simeq 2000$).

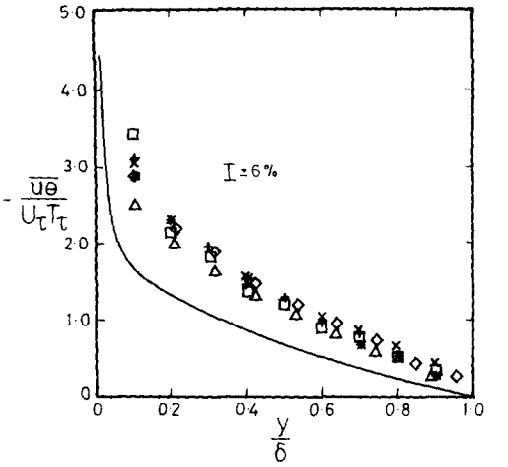

FIG. 17. Longitudinal heat flux distributions. Symbols are as in Fig. 5. ——, Fulachier.

present values by about 25–40%. To estimate Pr_t (Fig. 18), the gradient $\partial T/\partial U$ was inferred directly from plots (Fig. 10) of T^* vs. U^*. Except for $R_m = 990$, it is difficult to detect any systematic R_m dependence due to the relatively large uncertainty ($\pm 20\%$) in estimating Pr_t.

Correlation coefficients R_{uv}, $R_{v\theta}$ and $R_{u\theta}$ (Fig. 19) are approx. constant in the region $0.2 < y/\delta < 0.7$ and do not exhibit any noticeable dependence on R_m. Although the present values of R_{uv} are in good agreement with the value of -0.44 commonly found in the literature, the agreement between published values of $R_{u\theta}$ and $R_{v\theta}$ is generally poor. The present values of $R_{v\theta}$ are identical to Chen's [37] values but about 50% smaller than those of Fulachier [20] and Orlando *et al.* [28]. The present values of $R_{u\theta}$ are about 30% greater than Chen's [37] values and about 50% larger than Fulachier's values.

The structure parameter $a_{1\theta}$ [$\equiv \overline{v\theta}/\theta' (-\overline{uv})^{1/2}$] (Fig. 20) is constant, for $R_m > 990$, approx. equal to 0.5. For comparison, Bradshaw and Ferriss [38] and Fulachier [20] obtained values of 0.45 and 0.75 respectively. Another structure parameter is the ratio $\overline{u^2}/\overline{v^2}$, also shown in Fig. 20. This ratio is essentially

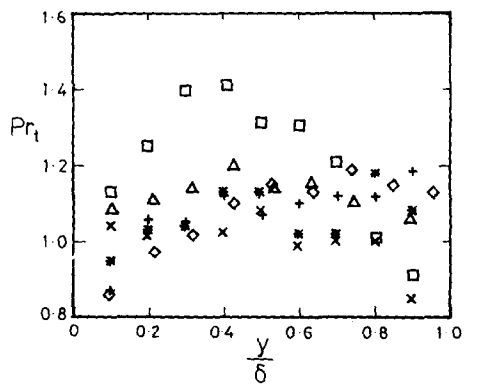

FIG. 18. Turbulent Prandtl number distributions. Symbols are as in Fig. 5.

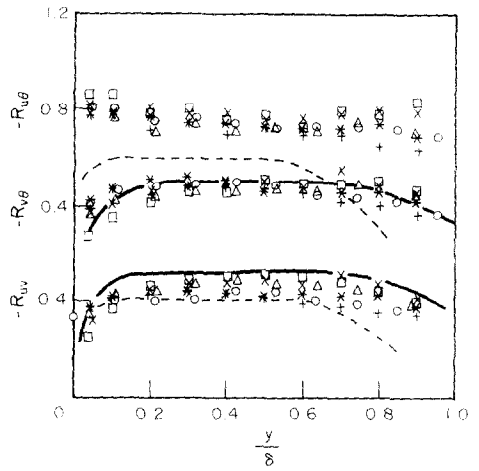

FIG. 19. Correlation coefficients R_{uv}, $R_{v\theta}$ and $R_{u\theta}$. Symbols are as in Fig. 1. – · – · –, Fulachier; ——, Chen.

independent of R_m except at $R_m = 990$ where its magnitude is rather large. Murlis *et al.*'s [6] measurement indicate only a slight R_m dependence for $R_m \geq 2000$. However, their R_m trend is opposite to the present one, and their values of $\overline{u^2}/\overline{v^2}$ are smaller than the present values by about 50%.

5. SUMMARY OF RESULTS

Measurements in the turbulent boundary layer on a smooth plate at zero pressure gradient indicate that, for both momentum and thermal fields, the law of the wall does not vary with Reynolds number. Constant values are found for κ, C and for the analogous parameters κ_θ and C_θ which appear in the logarithmic temperature distribution. The extent of the logarithmic velocity and temperature regions remains proportional to the boundary layer thickness when $R_m \geq 3100$. As a proportion of the boundary layer thickness, the extent of the velocity log-law and especially that for the temperature log-law increase as R_m decreases below 3100.

The influence of viscosity on the outer region of the boundary layer is reflected in the variation with R_m of the strengths of the velocity and thermal "wakes". The thermal wake strength is approx. one-half that for the velocity wake. However, mean velocity and mean temperature defect profiles are approximately independent of R_m in the outer layer. The deviation from the temperature log-law in the outer layer is reasonably well described by expressions analogous to those which describe the velocity wake. A linear relationship between mean temperature and mean velocity exists over a significant region of the layer at all R_m.

Profiles of r.m.s. temperature and longitudinal velocity fluctuations scale reasonably well with wall variables for $y^+ \lesssim 15$. Only approximate scaling on outer layer parameters is obtained when R_m is greater than about 3100. Correlation coefficients between velocity and temperature fluctuations do not appear to be strongly affected by R_m. The effect of R_m on the turbulent Prandtl number and on the turbulence structure parameter $a_{1\theta}$ is significant only at the smallest Reynolds numbers investigated. This latter result should be treated with caution since it reflects the relatively small measured values of the normal heat flux in the region close to the wall at these Reynolds numbers.

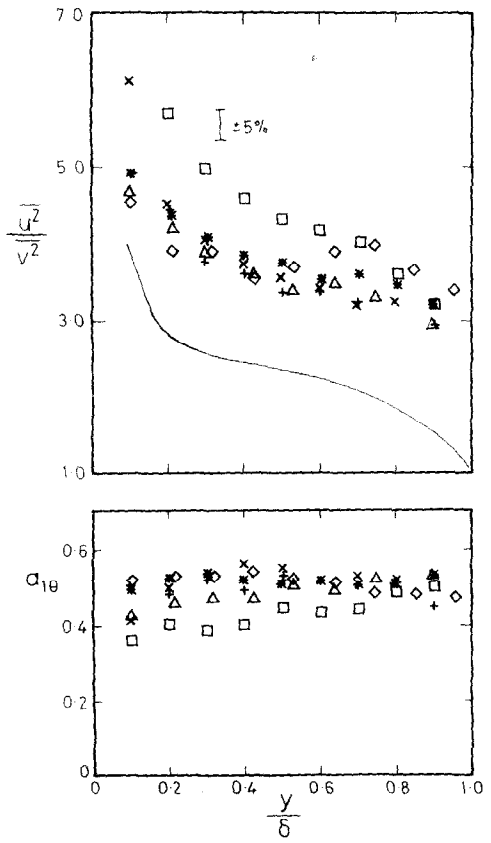

FIG. 20. Distributions of structure parameters $\overline{u^2}/\overline{v^2}$ and $a_{1\theta}$. Symbols are as in Fig. 5. ——, Klebanoff.

REFERENCES

1. D. E. Coles, The Turbulent Boundary Layer in a Compressible Fluid, *RAND Report* R-403-PR (1962).
2. R. L. Simpson, Characteristics of Turbulent Boundary Layers at Low Reynolds Numbers With and Without Transpiration, *J. Fluid Mech.* **42**, 769–802 (1970).
3. G. D. Huffman and P. Bradshaw, A Note on von Kármán's Constant in Low Reynolds Number Turbulent Flow, *J. Fluid Mech.* **53**, 45–60 (1972).
4. S. Corrsin and A. L. Kistler, Free Stream Boundaries of Turbulent Flows, *NACA Report* 1244 (1955).
5. P. Bradshaw, The Effect of Mean Compression or Dilation on the Turbulence Structure of Supersonic Boundary Layers, *J. Fluid Mech.* **63**, 449–464 (1974).
6. J. Murlis, H. M. Tsai and P. Bradshaw, The Structure of Turbulent Boundary Layers at Low Reynolds Number, submitted to *J. Fluid Mech.* (1980).
7. J. Murlis, The Structure of a Turbulent Boundary Layer at Low Reynolds Number, Ph.D. Thesis, Imperial College, University of London (1975).
8. L. P. Purtell, P. S. Klebanoff and F. T. Buckley, Turbulent Boundary Layer at Low Reynolds Number, *Phys. Fluids* **24**, 802–811 (1981).

9. L. P. Purtell, The Turbulent Boundary Layer at Low Reynolds Number, Ph.D. Thesis, University of Maryland (1978).
10. C. S. Subramanian, Some Properties of the Large Scale Structure in a Slightly Heated Turbulent Boundary Layer, Ph.D. Thesis, University of Newcastle, Australia (1981).
11. R. A. Antonia, A. Prabhu and S. E. Stephenson, Conditionally Sampled Measurements in a Heated Turbulent Jet, *J. Fluid Mech.* **72**(3), 455–480 (1975).
12. F. H. Champagne, The Temperature Sensitivity of Hot Wires, *Proc. Dynamic Flow Conference* (Edited by L. S. G. Kovasznay, A. Favre, P. Buchhave, L. Fulachier, B. W. Hansen), 101–114 (1979).
13. V. C. Patel, Calibration of the Preston Tube and Limitations on Its Use in Pressure Gradients, *J. Fluid Mech.* **23**, 185–208 (1965).
14. M. R. Head and V. Vasantha Ram, Simplified Presentation of Preston Tube Calibration, *Aeronaut. Q.* **12**, 295–300 (1971).
15. P. S. Klebanoff and Z. W. Diehl, Some Features of Artificially Thickened Fully Developed Turbulent Boundary Layers With Zero Pressure Gradient, *NACA Report* 1110 (1952).
16. J. M. R. Graham, The Development of the Turbulent Boundary Layer Behind a Transition Strip, Report 31492 FM4090, Aeronautical Research Committee (1969).
17. Q. A. Ahmad, R. E. Luxton and R. A. Antonia, Characteristics of a Turbulent Boundary Layer With an External Turbulent Uniform Shear Flow, *J. Fluid Mech.* **37**(2), 369–396 (1976).
18. J. C. Simonich and P. Bradshaw, Effect of Free Stream Turbulence on Heat Transfer Through a Turbulent Boundary Layer, *J. Heat Trans.* **100**, 671–677 (1978).
19. B. A. Kader and A. M. Yaglom, Heat and Mass Transfer Laws for Fully Turbulent Wall Flows, *Int. J. Heat Mass Transfer* **15**, 2329–2351 (1972).
20. L. Fulachier, Contribution à l'Etude des Analogies des Champs Dynamique et Thermique dans une Couche Limite Turbulente. Effet de l'Aspiration. Thèse Docteur ès Sciences, Université de Provence (1972).
21. A. M. Yaglom, Similarity Laws for Constant-Pressure and Pressure-Gradient Turbulent Wall Flows, *Ann. Rev. Fluid Mech.* **11**, 505–540 (1979).
22. A. E. Perry and P. H. Hoffmann, An Experimental Study of Turbulent Convective Heat Transfer From a Flat Plate, *J. Fluid Mech.* **77**, 355–368 (1976).
23. R. A. Antonia, H. Q. Danh and A. Prabhu, Response of a Turbulent Boundary Layer to a Step Change in Surface Heat Flux, *J. Fluid Mech.* **80**(1), 153–177 (1977).
24. J. Rotta, Ueber die Theorie der Turbulenten Grenzschlichten, *Mitt. Ström. Forsch. Nr. 1*, Max-Planck Institut (1950).
25. R. B. Dean, A Single Formula for the Complete Velocity Profile in a Turbulent Boundary Layer, *J. Fluid Engng* **98**, 723–726 (1976).
26. D. G. Mabey, Some Observations on the Wake Component of the Velocity Profiles of Turbulent Boundary Layers at Subsonic and Supersonic Speeds, *Aeronaut. Q.* **30**, 590–606 (1979).
27. A. E. Perry, J. B. Bell and P. N. Joubert, Velocity and Temperature Profiles in Adverse Pressure Gradient Turbulent Boundary Layers, *J. Fluid Mech.* **25**, 299–320 (1966).
28. A. F. Orlando, R. J. Moffat and W. M. Kays, Turbulent Transport of Heat and Momentum in a Boundary Layer Subject to Deceleration Suction and Variable Wall Temperature, Report HMT-17, Thermosciences Division, Department of Mechanical Engineering, Stanford University (1974).
29. M. M. Pimenta, R. J. Moffat and W. M. Kays, The Turbulent Boundary Layer. An Experimental Study of Transport of Momentum and Heat With the Effect of Roughness, Report HMT-21, Thermosciences Division, Department of Mechanical Engineering, Stanford University (1975).
30. B. F. Blackwell, W. M. Kays and R. J. Moffat, The Turbulent Boundary Layer on a Porous Plate. An Experimental Study of the Heat Transfer Behaviour With Adverse Pressure Gradients, Report HMT-16, Thermosciences Division, Department of Mechanical Engineering, Stanford University (1972).
31. A. E. Perry and C. J. Abell, Scaling Laws for Pipe-Flow Turbulence, *J. Fluid Mech.* **67**, 257–271 (1975).
32. P. Bradshaw, 'Inactive' Motion and Pressure Fluctuations in Turbulent Boundary Layers, *J. Fluid Mech.* **30**(2), 241–258 (1967).
33. A. E. Perry and C. J. Abell, Asymptotic Similarity of Turbulence Structures in Smooth and Rough Walled Pipes, *J. Fluid Mech.* **79**(4), 785–799 (1977).
34. S. M. Henbest, K. L. Lim and A. E. Perry, The Structure of Turbulence in Axisymmetric and Flat Plate Flows, *Proc. 7th Australasian Conf. Hydraul. Fluid Mech. Brisbane*, 172–174 (1980).
35. P. S. Klebanoff, Characteristics of Turbulence in a Boundary Layer with Zero Pressure Gradient, *NACA Report* 1247 (1955).
36. J. Blom, An Experimental Determination of the Turbulent Prandtl Number in a Developing Temperature Boundary Layer, Ph.D. Thesis, Technical University of Eindhoven (1970).
37. C. H. P. Chen, Large Scale Motion in a Boundary Layer: A Study Using Temperature Contamination, Ph.D. Thesis, University of Southern California (1975).
38. P. Bradshaw and D. H. Ferriss, Calculation of Boundary Layer Development Using the Turbulent Energy Equation. IV. Heat Transfer With Small Temperature Differences, *Nat. Phys. Lab. Report* 1271 (1968).

EFFET DU NOMBRE DE REYNOLDS SUR UNE COUCHE LIMITE TURBULENTE FAIBLEMENT CHAUFFEE

Résumé—Des mesures sur une couche limite turbulente, faiblement chauffée, avec des origines essentiellement identiques pour les champs thermique et dynamique, montrent que les constantes dans les régions logaritmiques de vitesse et de température ne varient pas avec le nombre de Reynolds. L'étendue de ces régions, par rapport à l'épaisseur dce la couche limite, est approximativement constante et indépendante du nombre de Reynolds d'épaisseur de quantité de mouvement R_m, quand $R_m \gtrsim 3100$. L'écart à la loi logarithmique de température dans la couche externe est raisonablement bien décrit par des expressions analogues à celles qui décrivent le "sillage". La valeur maximale de cette déviation augmente avec R_m dans le domaine 990–4750, mais elle est approximativement constante pour $R_m > 4750$ et égale à environ la moitié de l'écart maximal de vitesse. Les distributions de moyennes quadratiques de vitesse et de température s'accordent modérement avec les variables pariétales dans la partie interne de la sous-couche pour tout R_m. Pour la zone externe, l'accord est à peu près obtenu quand $R_m \gtrsim 3100$. Le seul effet notable de R_m sur le nombre de Prandtl turbulent et sur les paramètres de la structure de turbulence est observé aux plus petits nombres de Reynolds étudiés.

DER EINFLUSS DER REYNOLDS-ZAHL AUF EINE SCHWACH BEHEIZTE TURBULENTE GRENZSCHICHT

Zusammenfassung — Messungen an einer schwach beheizten turbulenten Grenzschicht mit im wesentlichen identischen Anfangspunkten für Impuls- und thermische Felder zeigen, daß die Konstanten in den Bereichen, in denen Temperatur und Geschwindigkeit einen logarithmischen Verlauf haben, sich mit der Reynolds-Zahl nicht ändern. Die Ausdehnung dieser Gebiete im Verhältnis zur Grenzschichtdicke ist näherungsweise konstant, unabhängig von der mit der Impulsgrenzschichtdicke gebildeten Reynolds-Zahl Re_m, wenn $Re_m \gtrsim 3100$ ist. Die Abweichung vom logarithmischen Verlauf der Temperatur in der äußeren Schicht wird annehmbar gut durch zum Geschwindigkeits-Nachstrom analoge Ausdrücke beschrieben. Der maximale Wert dieser Abweichung nimmt mit Re_m im Bereich von 990 bis 4750 zu, ist aber näherungsweise konstant bei $Re_m > 4750$, und etwa gleich der halben maximalen Geschwindigkeitsabweichung. Die Verteilungen der quadratischen Mittelwerte von Geschwindigkeit und Temperatur verhalten sich ungefähr entsprechend den Wandvariablen im inneren Teil der Unterschicht bei allen Re_m. Der Bezug auf die Variablen der äußeren Strömung ist nur näherungsweise möglich, wenn $Re_m \gtrsim 3100$ ist. Der einzige nennenswerte Effekt von Re_m auf die turbulente Prandtl-Zahl und die Strukturparameter der Turbulenz wird bei der kleinsten untersuchten Reynolds-Zahl beobachtet.

ВЛИЯНИЕ ЧИСЛА РЕЙНОЛЬДСА НА СЛЕГКА НАГРЕТЫЙ ТУРБУЛЕНТНЫЙ ПОГРАНИЧНЫЙ СЛОЙ

Аннотация — Результаты измерений, проведенных в слегка нагретом турбулентном пограничном слое при почти одинаковых значениях виртуального начала динамического и температурного полей, показывают, что константы в скоростной и температурной логарифмических областях не изменяются с изменением числа Рейнольдса. Протяженность этих областей относительно толщины пограничного слоя почти не меняется и не зависит от числа Рейнольдса R_m, рассчитанного по толщине потери импульса при $R_m \gtrsim 3100$. Отклонение от температурного логарифмического закона во внешней области довольно хорошо описывается выражениями, которые аналогичны зависимостям, используемым для описания скоростного "следа". Максимальное значение этого отклонения возрастает с увеличением числа R_m в диапазоне 990–4750, но остается почти постоянным при $R_m > 4750$ и приблизительно равным половине максимального отклонения скорости. Распределение среднеквадратичных значений пульсаций скорости и температуры во внутренней области подслоя, нормированных параметрами на стенке, практически универсально при всех значениях R_m. Универсальность распределения характеристик во внешней части подслоя достигается только при $R_m \gtrsim 3100$. Заметное влияние числа R_m на турбулентное число Прандтля и параметры структуры турбулентности отмечается только при самых малых исследованных значениях числа Рейнольдса, достигнутых в настоящем эксперименте.